



# Structuring a multi-nodal neural network *in vitro* within a novel design microfluidic chip

Rosanne van de Wijdeven<sup>1</sup> · Ola Huse Ramstad<sup>2</sup> · Ulrich Stefan Bauer<sup>2</sup> · Øyvind Halaas<sup>1</sup> · Axel Sandvig<sup>2,3,4</sup> · Ioanna Sandvig<sup>2</sup>

Published online: 2 January 2018

© Springer Science+Business Media, LLC, part of Springer Nature 2017

## Abstract

Neural network formation is a complex process involving axon outgrowth and guidance. Axon guidance is facilitated by structural and molecular cues from the surrounding microenvironment. Micro-fabrication techniques can be employed to produce microfluidic chips with a highly controlled microenvironment for neural cells enabling longitudinal studies of complex processes associated with network formation. In this work, we demonstrate a novel open microfluidic chip design that encompasses a freely variable number of nodes interconnected by axon-permissible tunnels, enabling structuring of multi-nodal neural networks *in vitro*. The chip employs a partially open design to allow high level of control and reproducibility of cell seeding, while reducing shear stress on the cells. We show that by culturing dorsal root ganglion cells (DRGs) in our microfluidic chip, we were able to structure a neural network *in vitro*. These neurons were compartmentalized within six nodes interconnected through axon growth tunnels. Furthermore, we demonstrate the additional benefit of open top design by establishing a 3D neural culture in matrigel and a neuronal aggregate 3D culture within the chips. In conclusion, our results demonstrate a novel microfluidic chip design applicable to structuring complex neural networks *in vitro*, thus providing a versatile, highly relevant platform for the study of neural network dynamics applicable to developmental and regenerative neuroscience.

**Keywords** Microfabrication · Maskless aligner · Lab-on-chip · Axon growth and guidance · 3D cell culture · Organoid

## 1 Introduction

The use of microfabrication techniques to create lab-on-chip platforms and biosensors has facilitated biomedical research in many areas. In the last two decades, various types of

microfluidic chips have emerged as a research platform for neuronal cells (Dollé et al. 2013; Park et al. 2006; Taylor et al. 2003). These chips are commonly made of polydimethylsiloxane (PDMS), a transparent biocompatible material (Whitesides 2006). Customized chips can be readily designed and fabricated. Compared to standard culture vessels, tailored microfluidic chips enable physical confinement of cell cultures, as for example neural networks, by compartmentalization. Furthermore, multiple cell compartments may be interconnected via miniature channels ( $\mu\text{m}$ -scale) only permissible to axons, thus providing high spatial control of neuronal axons and somata (Ravula et al. 2007; Taylor et al. 2003; Vahidi et al. 2008). In this way, the tunnels isolate axons from their somata, which provides a unique possibility to directly study as well as influence axon guidance mechanisms (Taylor et al. 2005).

Tailoring the design of a microfluidic chip so that multiple subpopulations of cells can become interconnected provides a reductionist, yet realistic *in vitro* approximation of structural and functional elements of *in vivo* neural networks (Sporns and Kötter 2004). Such *in vitro* neural networks are amenable to specific manipulations influencing connectivity and can thus provide a valid platform for studying neural mechanisms that may

---

Rosanne van de Wijdeven and Ola Huse Ramstad share first authorship

✉ Rosanne van de Wijdeven  
Rosanne.v.d.wijdeven@ntnu.no

<sup>1</sup> Department of Clinical and Molecular Medicine, Faculty of Medicine and Health Sciences, Norwegian University of Science and Technology, PO Box 8905 MTF, NO-7491 Trondheim, Norway

<sup>2</sup> Department of Neuromedicine and Movement Science, Faculty of Medicine and Health Sciences, Norwegian University of Science and Technology, N-7491 Trondheim, Norway

<sup>3</sup> Department of Pharmacology and Clinical Neurosciences, Division of Neuro, Head and Neck, Umeå University Hospital, SE-90187 Umeå, Sweden

<sup>4</sup> Department of Neurology and Clinical Neurophysiology, St Olavs Hospital, 7030 Trondheim, Norway

otherwise be difficult to observe *in vivo* or in standard *in vitro* assays. For example, inducing axonal injury or incorporating patient-derived morphogenetically engineered neurons within the microfluidic devices, enables modelling pathophysiological features of central nervous system (CNS) lesions, including neurodegenerative diseases (Deleglise et al. 2014; Hosmane et al. 2011; Lu et al. 2012; Poon et al. 2011; Taylor et al. 2005; Wang et al. 2017). Additionally, the compatibility of microfluidic chips with microscopy, optogenetics (Lee et al. 2016; Renault et al. 2015), multi-electrode arrays (Kanagasabapathi et al. 2011) and other biosensors such as cyclic voltammetry (Chuang et al. 2013; Yu et al. 2016) highlights their potential as a multifunctional research platform, applicable to many areas of neuroscience.

In this study, we designed, fabricated and tested two novel microfluidic chips comprised of four and six compartments interconnected by axon-permissible tunnels designed to promote directional axonal outgrowth. We describe the design, fabrication and application of the chips. We show that we could structure a neural network consisting of six smaller networks *in vitro*. Furthermore, we conducted an experiment to test the compatibility of the chip with 3D dorsal root ganglion (DRG) cultures in Matrigel, a gel consisting of extracellular matrix components, mimicking the *in vivo* microenvironment (Kleinman and Martin 2005). The 3D DRG cultures in Matrigel within the chip were readily established due to the open structure of the chip. Neural networks of a 3D culture has an increased structural and connective complexity as compared to 2D cultured neural networks, and therefore a closer recapitulation of an *in vivo* neural network. Similarly, we demonstrate the compatibility of the chip design with organoid-like cell culture (neuronal aggregate), a 3D cell culture model based on the self-organization of induced pluripotent stem (iPS) cell-derived neurons and microlevel recapitulation of neural structures (Lancaster et al. 2017).

## 2 Method and materials

### 2.1 Design

The microfluidic design in this study comprises multiple cell compartments, interconnected by funnel-shaped micrometre-sized tunnels. The cell compartments are almost entirely open on top, i.e. they are not enclosed within the chip, allowing easy access for cell seeding and culture media and reagent handling. The areas where the compartments connect to the tunnels are enclosed within the microfluidic chip. Hereafter we define the open area in the cell compartments as *seeding wells* and the enclosed area as the *active sites* (Fig. 1b). The tunnels are 700  $\mu\text{m}$  long and are specially designed to provide directionality for outgrowing axons. Specifically, the tunnels are 15  $\mu\text{m}$  wide at one end, however at about  $\frac{1}{4}$  of their length, (Peyrin et al. 2011) they split up to smaller, 5  $\mu\text{m}$ -wide tunnels connecting

with the opposite compartment. Thus, axonal ingrowth at the narrow end is deterred by the small tunnel openings (data not shown). Combined the cell compartment, active zone and funnel-shaped micro-sized tunnels are defined as a node.

Two types of microfluidic chips are described in this study, i.e. chips encompassing either 4 or 6 nodes (Fig. 2a, b). The 4-nodal microfluidic chip incorporates similar features to those of the 6-nodal chip (Fig. 1a) except for the fact that the seeding wells have a larger diameter (6 mm). This makes the 4-nodal chip suitable for organoid- and organotypic slice culture experiments. The 6-nodal microfluidic chip is designed to enable structuring complex multi-nodal neural networks *in vitro*. Our photoresist moulds are fabricated employing a maskless aligner, thus either chip design can be adjusted to meet assay-specific requirements.

### 2.2 Fabrication

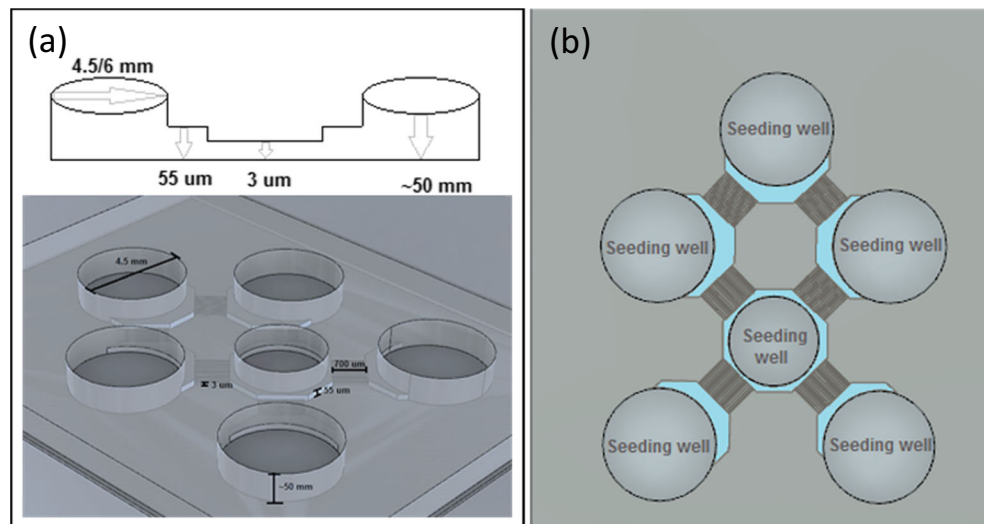
#### 2.2.1 Fabrication of the mould

The mould, i.e. the photoresist pattern used to create the microfluidic chip, was fabricated in a two-step photolithography process employing SU8 series photoresist (Microchem), a spin coater (spin150, SPS-Europe B.V.), a hotplate and a maskless aligner (Heidelberg Instruments, MLA150). MrDev 600 (micro resist technology GmbH) was used to develop the mould. SU-8 2 was spin-coated onto a 2" Silicon wafer (Siltronix) according to a two-step program, at 500 rpm for 5 s (300 rpm/min) and 1500 rpm for 30 s (300 rpm/min). After a two-step soft bake at 65 °C for 1 min and, subsequently 95 °C for 3 min, the film was exposed to a laser of 375 nm at a dosage of 2000  $\text{mJ}/\text{cm}^2$ . After a two-step post-exposure bake, i.e. 65 °C for 1 min, followed by 95 °C for 1 min, the first layer of the mould was developed for 1 min. A second layer of SU-8 3050 (MicroChem) was spin-coated at 500 rpm for 10 s (300 rpm/min) followed by 3000 rpm for 30 s (300 rpm/min). After a soft bake at 95 °C for 15 min, the film was exposed at 6000  $\text{mJ}/\text{cm}^2$  (375 nm). The film was baked at 65 °C for 1 min and at 95 °C for 4 min. Following a 5–8 min development, the film was hard baked at 95 °C for 3 min. A surface profile of the final pattern with a Profilometer (Dektak 150, Veeco) confirmed the intended heights of 5  $\mu\text{m}$  and 55  $\mu\text{m}$  respectively for the first and second layer.

#### 2.2.2 Fabrication of the microfluidic chip

Prior to the fabrication of the microfluidic chips, the mould was silanized (trichloro(1H,1H,2H,2H-perfluorooctyl (97%), Sigma Aldrich) in vacuum for 2 h to prevent detachment of the photoresist from the wafer when peeling off the PDMS microfluidic chip from its mould. A suspension of silicone elastomer and a curing agent (10:1) (SYLGARD®184 elastomer kit, Dow Corning) was mixed, degassed and then cast onto the mould. The microfluidic chip was cured in an oven (TS 8056, Termaks)

**Fig. 1** **a** Structural features and relevant dimensions within the microfluidic chip. **b** Top view image of the microfluidic chip (6-nodal) with the enclosed active areas indicated in blue



at 65 °C for 4 h, and afterwards carefully peeled from the mould. The cell compartments in the chips were manually punched out (Ø 6 mm 4-nodal chip and 4.5 mm 6-nodal chip). After removing PDMS debris from the chips with scotch tape, each chip was immersed in acetone and ethanol (70%) and sonicated for 10 min each. The chips were then left to dry overnight. In addition, coverslips (24 × 32 mm Menzel-Gläser and 22 × 22 mm, VWR International) were immersed in 70% ethanol and left to dry overnight. Both the PDMS devices and coverslips were treated with oxygen plasma (Femto, Diener Electronics) employing 80 sccm of O<sub>2</sub> flow at a pressure of 0.34 mbar and 80 W for 1 min. After carefully pressing the PDMS devices onto the coverslips, the microfluidic chips were heated at 70 °C for 30 s on a hotplate to finalize the bonding. Finally, the microfluidic chips were filled up with sterile water to maintain the hydrophilic surface of the PDMS.

## 2.3 Cells and materials

### 2.3.1 Primary dorsal root ganglia (DRGs) dissociation

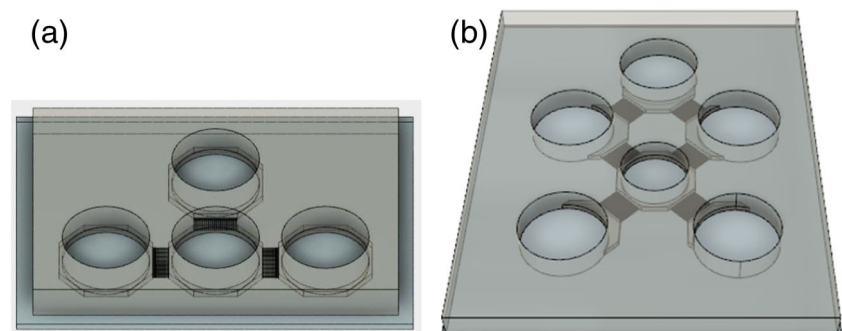
DRGs were obtained from adult Sprague Dawley rats. Briefly, following euthanasia with CO<sub>2</sub>, the vertebral column was excised, the lumbar and thoracic spinal cord segment exposed,

and the DRGs dissected out and placed in cold Hank's Balanced Salt Solution (HBSS) (Gibco). The DRGs were subsequently transferred to a warm dissociation solution containing 50% Dispase-2 (Merck-Millipore), 25% DNase (Sigma) and 25% Collagenase-1 (MP Biomedicals) and agitated continuously for 45 min. Following dissociation, the cells were centrifuged at 80 x g and subsequently seeded on a 6-well plate coated with laminin (B521, Biolamina) in DRG media, in which they were maintained until seeding into the chips.

### 2.3.2 DRG cell culture in the microfluidic chip

Microfluidic chips were coated with poly-L-ornithine (Sigma) diluted in cell culture-grade distilled water (20 μg/mL) and incubated at 37 °C for 4 h. Chips were afterwards washed with cell culture-grade distilled water and coated with laminin (B521, Biolamina) diluted in phosphate buffered saline (PBS) (5 μg/mL) and incubated at 37 °C for 2 h. The laminin was subsequently replaced with culture media consisting of Neurobasal medium, with 2% B27, 2 mM Glutamax, 5% fetal bovine serum, and 10 μg/mL insulin and allowed to equilibrate in an incubator at 37 °C one day prior to cell seeding. Unless stated otherwise, all products were purchased from Thermo Fisher Scientific.

**Fig. 2** **a** Illustration of the design of the 4-nodal microfluidic chip. **b** Illustration of the design of the 6-nodal microfluidic chip



The cells were seeded in the 6-nodal chip, and the seeding proceeded as follows: DRGs cultured in a 6-well plate were passaged with 0.25% Trypsin/EDTA and centrifuged at 200 x g. The DRGs were re-suspended at a concentration of 1800 cells/ $\mu$ L. 10  $\mu$ L of media in each cell compartment of the chips were then aspirated and simply replaced with 10  $\mu$ L cell suspension in the centre of each cell compartment. The DRG neurons were thus plated at a density of 18,000 cells per compartment. Two thirds of the media was replaced in each compartment 4 h post-seeding, and every second day afterwards.

### 2.3.3 Cell staining

Neural network formation proceeded for 14 days in chip (DIC). Following completion of network formation, the cultures were fixed with 2% paraformaldehyde (PFA) directly, without disruptive prior washes, in cell culture media for 15 min. Additionally, 4% PFA was added to each cell compartment after aspirating the previous solution, and the cells incubated for another 10 min prior to immunocytochemistry (ICC). For ICC, the cells were washed three times with PBS, and incubated for 2 h at RT in blocking solution containing 5% goat serum and 0.3% Triton X in PBS, followed by incubation with anti-Tuj-1 mouse monoclonal primary antibody (1:1000; Abcam) overnight at 4 °C. The following day, the cells were washed three times with PBS, before incubation with a goat anti-mouse Alexa<sup>®</sup> 488 secondary antibody for 3 h at RT and counterstaining with Hoechst (during the last 5 min). After three washes with PBS, cells were incubated for 40 min with Phalloidin 647, a conjugate f-actin stain (unless stated otherwise all secondary antibodies were purchased from Thermo Fisher Scientific). The chips were kept in PBS post staining and imaged the following day.

Chips were imaged with a Zeiss Axio Vert.A1 Microscope and Zeiss LSM 510 Meta Confocal. All image processing was performed in ImageJ (NIH).

### 2.3.4 3D cultures within the microfluidic chip

DRGs were cultured in 3D in the 6-nodal chip to test the compatibility of our design with such cultures. 3D DRG cultures were established in the microfluidic chips using Matrigel (hESC-qualified, Corning). Prior to seeding, the chips were coated with Matrigel, meanwhile the chips were kept in a petridish on ice to maintain a low viscosity of the Matrigel enabling flow into the enclosed active sites of the chip. Following incubation at 37 °C for 2 h, DRGs were seeded into the Matrigel according to the cell seeding procedure described above.

### 2.3.5 Neuronal aggregate culture in the microfluidic chip

Motor neuron aggregates were derived from ChiPS18 Human iPS line (Takara Bio). ChiPS18 cells were expanded in

adherent cell culture on cell culture vessels coated with 5  $\mu$ g/ml laminin 521 (B521, Biolamina) diluted in DPBS, calcium, magnesium and stored at 4 °C overnight. Cells were seeded in media containing KnockOut DMEM/F-12 media, 20% CTS KnockOut serum replacement XenoFree, 2 mM Glutamax, 1% EmbryoMax MEM Non Essential Amino Acids (Millipore), 50 U/ml Penicillin-Streptomycin, 55  $\mu$ M 2-Mercaptoethanol (Sigma), 4 ng/ml FGF basic recombinant human (Peprotech) and 20  $\mu$ M Y-27632 (Sigma). Media were changed every 24 h. Replacement media after seeding contained no Y-27632. Cells were allowed to expand to 85–90% confluence before harvesting with 0.25% Trypsin/EDTA and pelleted by centrifugation at 200 xg. Cells were differentiated using an adapted version of the neutralised motor neuron differentiation protocol described in Amoroso et al. 2013 without being dissociated as the final step (Amoroso et al. 2013).

Microfluidic chips were coated with poly-L-ornithine (Sigma) diluted in cell culture-grade distilled water (20  $\mu$ g/mL) and incubated at 37 °C for 4 h. Chips were subsequently washed with cell culture-grade distilled water and coated with natural mouse laminin (10  $\mu$ g/mL) diluted in Leibovitz's L-15 Medium supplemented with 1.9 mg/ml sodium bicarbonate and incubated at 37 °C for 4 h. Before seeding, the laminin was replaced with motor neuron culture media consisting of Neurobasal medium, 2 mM Glutamax, 1% EmbryoMax MEM Non Essential Amino Acids (Millipore), 50 U/ml Penicillin-Streptomycin, 1% N2 Supplement, 2% B27 minus antioxidants, 0.4  $\mu$ g/mL Ascorbic acid, 25  $\mu$ M L-glutamic acid HCl (Sigma), 25  $\mu$ M 2-Mercaptoethanol (Sigma), 1  $\mu$ M All-trans retinoid acid (Sigma), 20  $\mu$ M Y-27632 (Sigma) and allowed to equilibrate at 37 °C, 5% CO<sub>2</sub> overnight. Neuronal aggregates were carefully seeded using a 5 ml serological pipette and their position in the cell compartment adjusted using an extra-long 200  $\mu$ l pipette tip. 3/4 media changes were carried out every 48 h. Neuronal aggregates were allowed to develop motor neuron networks for 21 DIC before being fixed and stained as described in Section 2.3.3. In addition to the stains used on the DRGs, cells were incubated with primary antibodies for rabbit monoclonal synaptophysin (1:50 Abcam), while chicken polypeptide neurofilament heavy (1:1000 Abcam) was used instead of phalloidin. Alexa 488 anti-rabbit, 568 anti-mouse and 647 anti-chicken were used as the secondary antibodies following a short 5 min incubation with Hoechst.

## 3 Results/discussion

### 3.1 Structuring the neural network within the microfluidic chip

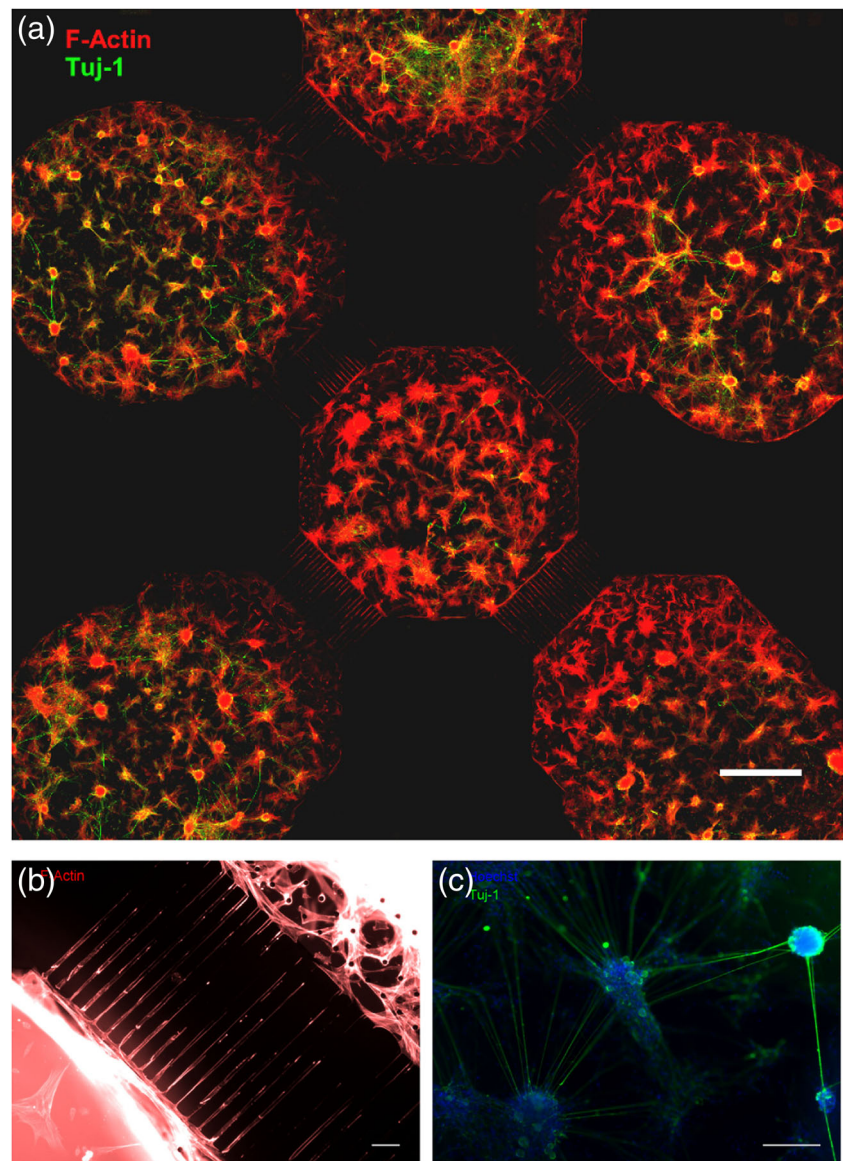
DRGs are pseudo-unipolar cells with afferent sensory axons, which precludes interconnectivity. However, the rapid outgrowth of DRG axons makes them an appealing choice of cell

type for a proof-of- concept study. Within 24 h of seeding, the primary DRGs started migrating out of the seeding wells into the active sites of the microfluidic chip. At 3 DIC, DRGs in the active site started extending axons into the tunnels. Over the next 11 days, axon outgrowth into the tunnels increased and axons started reaching networks in the opposite compartments (Fig. 3b). At 14 DIC the cells within the chips were fixed and stained for F-actin Tuj-1 and Hoechst (Fig. 3a, b, c). An observation period of 14 DIC was chosen to provide a timeframe long enough for axons to extend into the tunnels and cross to the opposite cell compartment. To our knowledge, this is the first time a microfluidic chip has been used to structure a neural network *in vitro* that encompasses six interconnected nodes (Fig. 3a). The higher number of nodes allows for a more complex neural network *in vitro*, thus recapitulating some of the complexity lost from *in vivo* networks.

Furthermore, the flexibility of our design allows assay-specific configurations by adjusting the number of nodes and/or length and directionality of the tunnels, thus providing a highly versatile platform for structuring complex networks.

Previous studies have shown, with different cell types, that less than a week was sufficient for axons to cross tunnels from the original compartment to the other side (Lei et al. 2016; Zahavi et al. 2015). In our study, twice as much time was required for axons to reach opposite nodes. Apart from the different cell type used, the length of the axon tunnels in previous studies was shorter (Lei et al. 2016, Zahavi et al. 2015), i.e. 300  $\mu\text{m}$  and 450  $\mu\text{m}$ , compared to the 700  $\mu\text{m}$  length used in our design. Furthermore, the increased complexity of our design, incorporating six interconnected compartments, might additionally influence the time required for axons to cross between compartments. This may be attributable to diffusion

**Fig. 3** **a** Tiled composite immunofluorescence image from a confocal microscope of the structured DRG network stained for Tuj-1 and F-Actin (scale bar: 1000  $\mu\text{m}$ ). **b** Magnified image of one of the active zones and axon tunnels, showing axons that have entered the tunnels, some of which have crossed to the opposite compartment (scale bar: 50  $\mu\text{m}$ ). **c** ICC image of DRGs within the seeding well forming interconnected clusters; Tuj-1 (green), Hoechst (blue). (scale bar: 50  $\mu\text{m}$ )



of signalling cues between multiple compartments, resulting in a more complex microenvironment for axon guidance. One limitation of the presented fabrication protocol of the microfluidic chip is the irreversible bonding of the chip to the glass coverslip. This can present a challenge during ICC procedures, as antibodies may not easily reach inside the tunnels, which may decrease the efficiency of the ICC protocol for staining outgrowing axons. This may necessitate long exposure under fluorescence imaging to enable visualization of the immunostained axons within the tunnels (Fig. 3).

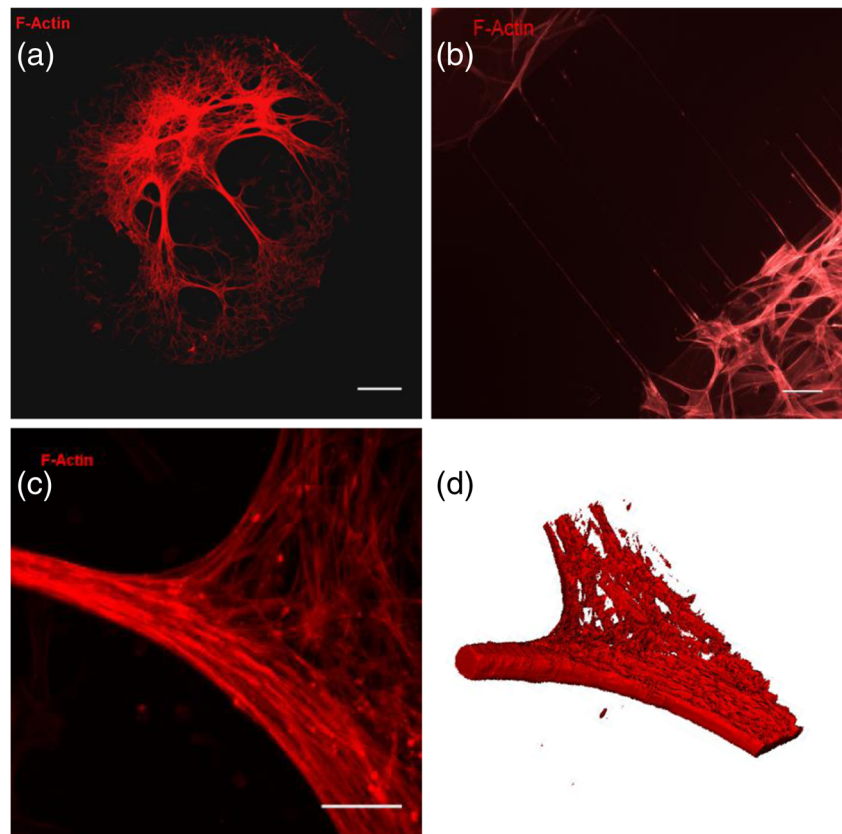
### 3.2 Mimicking *in vivo* neural networks *in vitro*

Considering the 3D nature of the *in vivo* extracellular microenvironment, 3D cultures provide a more analogous *in vitro* emulation of the relevant extracellular dynamics than 2D cultures. Therefore, we tested the applicability of the 6-nodal microfluidic chips to 3D neuronal cultures using Matrigel to mimic the *in vivo* extracellular microenvironment. Matrigel is a hydrogel preparation containing basement membrane proteins, which provides structural and biochemical cues similar to the extracellular matrix (ECM) (Kleinman and Martin 2005). In our study, DRG culture in Matrigel resulted in 3D structured neural networks within the cell compartments (Fig. 4 a, b, c, d). In the 3D cultures, we observed that the duration necessary for the axons to reach and interconnect

with opposite nodes was longer than for 2D cultures, i.e. 28 DIC as opposed to 14 DIC. It is a reasonable assumption to make that the embedded microarchitecture of the chip, combined with the 3D gel ECM influence chemotaxis within the chip by slower diffusion of signalling molecules between the different nodes, thus providing complex cues for axon guidance and, by the same token, neural network formation. Therefore, by applying a versatile multi-nodal microfluidic chip design such as the one presented here, and by modulating chemical and/or rheological properties of the ECM, we can influence neural network dynamics within the chip.

Another advantage of our design is that it encloses the active sites while leaving the cell compartments mostly ‘open’ (Fig. 1a, b), thus enabling access to the cells and ease of handling especially when introducing highly viscous substances, such as Matrigel, into the microfluidic chip. Apart from ease of creating 3D cultures, the ‘open cell compartment’ design of the microfluidic device has the added benefit of enabling more control over the seeding reproducibility in terms of number of cells seeded in each compartment. Importantly, the design bypasses the necessity of seeding cells via inlet and outlet channels commonly used in other microfluidic chips (Taylor et al. 2005), and thus allows direct seeding into the well, preventing cell damage due to shear stress as well as the flushing out of cells through outlets. In addition, avoiding the incorporation of such channels into the microfluidic chip results in

**Fig. 4** Images from a DRG 3D culture in matrigel within the microfluidic chip, taken with a confocal microscope. **a** Tiled image of the 3D DRG culture within one compartment. Axon outgrowth towards an opposite node can be seen in the top right corner. Scale bar represents 500  $\mu\text{m}$ . **b** magnified image of axon outgrowth in tunnels. Scale bar: 100  $\mu\text{m}$ . **c** magnified image of a DRG axonal tract in 3D. Scale bar represents 100  $\mu\text{m}$ . **d** Z-stack image of the same axonal tract



an easy-to-use, adjustable platform, which can be readily adopted by standard neuroscience laboratories. The open structure microfluidic chip has been demonstrated in recent studies (Lee et al. 2016; Renault et al. 2015; Zahavi et al. 2015). However, in contrast with previous demonstrated designs, ours contains more cell compartments. In terms of microfabrication, excluding inlet and outlet channels from the design increases the possible number of cell compartments that can fit within the microfluidic chip using the applied microfabrication techniques. A higher number of interconnected nodes enable structuring more complex multi-nodal networks, including networks comprising different neuronal types, thus providing a superior platform for recapitulating emerging dynamics of *in vivo* neural networks. Furthermore, previously reported microfluidic chip designs incorporate a border between the open and the enclosed area, which is difficult to image with standard bright field microscopy due to light diffraction at the edges. Our designs, however, circumvents this issue by incorporating an active zone (Fig. 1a), i.e. an area that enables the visualisation of ‘active’ neurons involved in axon outgrowth towards opposite compartments.

### 3.3 Neuronal aggregate culture on a chip

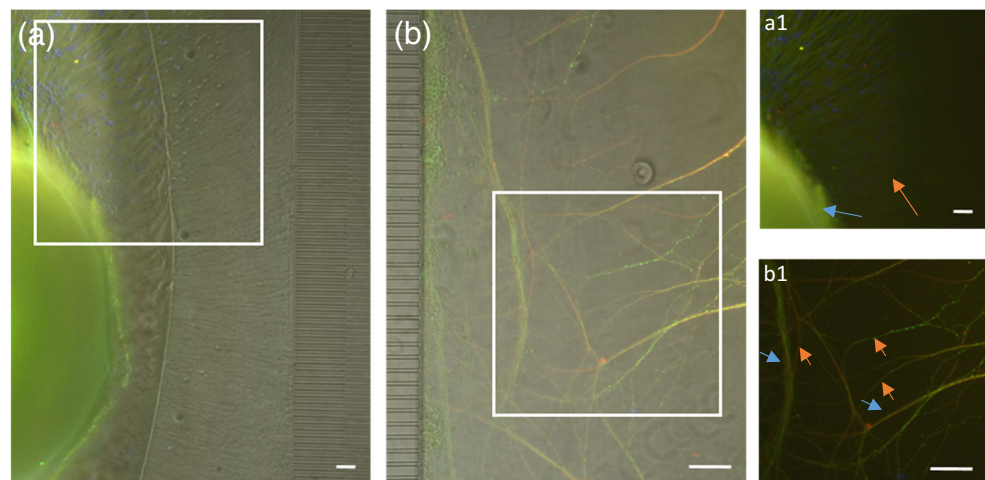
Organoids, as well as cell-specific neuronal aggregates, have in recent years become another *in vitro* platform for mimicking *in vivo* cellular dynamics in normal and perturbed conditions. Interestingly, self-organising neuronal aggregates of engineered neuronal subtypes can give rise to highly complex plastic networks. We therefore wanted to test the compatibility of our chip design as a platform for neuronal aggregate culture. To this end, we seeded motor neuron aggregates in the outer cell compartments of the 4-nodal microfluidic chip (Fig. 5a, a1). We observed the first axons growing into the tunnels by 2 DIC, while by 3 DIC, we could observe axons exiting the tunnels at the other end and entering the opposite

compartment. We further observed that axons exiting the tunnels initially formed a dense bundle and subsequently separated and extended towards the centre of the opposite compartment (Fig. 5b, b1), consistent with axon fasciculation and defasciculation as part of axonal pathfinding (Tessier-Lavigne et al. 1988) (Fig. 5b, b2). The neuronal aggregates used in this study had diameters of >1 mm and could be directly placed into an active site within the chip due to the open compartment design. We can thus demonstrate the advantage of our design over chips that employ inlet and outlet channels for cell seeding when it comes to this increasingly relevant complex form of 3D cell culture.

## 4 Conclusions

In this study, we demonstrated the applicability of a novel, versatile microfluidic chip design for structuring multi-nodal neural networks *in vitro*. Furthermore, we showed that the chip enables 3D neural network culture, including culture of neuronal aggregates. Apart from the above, an added advantage of the chip is that its partially open design allows a high level of control over, and thereby, reproducibility of cell seeding, while it reduces the risk of flow-induced shear stress on the cells. Moreover, the interconnected nodes within the chip and directional control provided by funnelling tunnels facilitate improved *in vitro* recapitulation of *in vivo* neural networks. As such, these microfluidic chips provide a highly promising novel *in vitro* modelling platform applicable to studies of axon growth and guidance relevant to neural network development, damage and regeneration (Taylor et al. 2005; Taylor et al. 2015; Tsantoulas et al. 2013; Zahavi et al. 2015). The next step in developing this design is the incorporation of a multi-electrode array (MEA) interface within the nodes, enabling electrophysiological measurements and/or modulation.

**Fig. 5** Composite ICC phase contrast images of axon outgrowth from a motor neuron aggregate at 21 DIC. **a** Axons extending (orange arrow) from the neural aggregate (blue arrow) in the seeding well (**a1**) into the active zone and axon tunnels. **b** Fasciculated (blue arrows) and defasciculated (orange arrows) axons entering the opposite compartment (**b1**); Neurofilament heavy (red), Synaptophysin (green), Hoechst (blue), Tuj-1 (yellow). Scalebars represents 100  $\mu\text{m}$



**Acknowledgements** This work was supported by the Research Council of Norway, Norwegian Micro- and Nano-Fabrication Facility, NorFab, project number 245963/F50, NTNU program for Enabling Technologies, (Nanotechnology), and the Liaison Committee between the Central Norway Health Authority and NTNU (Samarbeidsorganet HMN-NTNU).

**Compliance with ethical standards** All animal procedures were in accordance with the EU Directive 86/609/EEC and the Norwegian laws and regulations controlling procedures on experimental animals.

**Conflict of interest** There are no conflicts to declare.

## References

- M.W. Amoroso, G.F. Croft, D.J. Williams, S. O’Keeffe, M.A. Carrasco, A.R. Davis, et al., *J Neurosci : Official J Soc Neurosci.* **33**, 2 (2013)
- M.-C. Chuang, H.-Y. Lai, J.-A. Annie Ho, Y.-Y. Chen, *Biosens. Bioelectron.* **41** (2013)
- B. Deleglise, S. Magnifico, E. Duplus, P. Vaur, V. Soubeyre, M. Belle, et al., *Acta Neuropathol. Commun.* **2** (2014)
- J.-P. Dollé, B. Morrison, R.R. Schloss, M.L. Yarmush, *Lab Chip* **13**, 3 (2013)
- S. Hosmane, A. Fournier, R. Wright, L. Rajbhandari, R. Siddique, I.H. Yang, et al., *Lab Chip* **11**, 22 (2011)
- T.T. Kanagasabapathi, D. Ciliberti, S. Martinoia, W.J. Wadman, M.M.J. Decré, *Front. Neuroeng.* **4** (2011)
- H.K. Kleinman, G.R. Martin, *Semin. Cancer Biol.* **15**, 5 (2005)
- M.A. Lancaster, N.S. Corsini, S. Wolfinger, E.H. Gustafson, A.W. Phillips, T.R. Burkard, et al., *Nat. Biotechnol.* **35**, 7 (2017)
- H.U. Lee, S. Nag, A. Blasiak, Y. Jin, N. Thakor, I.H. Yang, *ACS Chem. Neurosci.* **7**, 10 (2016)
- Y. Lei, J. Li, N. Wang, X. Yang, Y. Hamada, Q. Li, et al., *Integr. Biol.* **8**, 3 (2016)
- X. Lu, J.S. Kim-Han, K.L. O’Malley, S.E. Sakiyama-Elbert, *J. Neurosci. Methods* **209**, 1 (2012)
- J.W. Park, B. Vahidi, A.M. Taylor, S.W. Rhee, N.L. Jeon, *Nat. Protoc.* **1**, 4 (2006)
- J.-M. Peyrin, B. Deleglise, L. Saias, M. Vignes, P. Gougis, S. Magnifico, et al., *Lab Chip* **11**, 21 (2011)
- W.W. Poon, M. Blurton-Jones, C.H. Tu, L.M. Feinberg, M.A. Chabrier, J.W. Harris, et al., *Neurobiol. Aging* **32**, 5 (2011)
- S.K. Ravula, M.S. Wang, S.A. Asress, J.D. Glass, A. Bruno Frazier, *J. Neurosci. Methods* **159**, 1 (2007)
- R. Renault, N. Sukenik, S. Descroix, L. Malaquin, J.-L. Viovy, J.-M. Peyrin, et al., *PLoS One* **10**, 4 (2015)
- O. Sporns, R. Kötter, *PLoS Biol.* **2**, 11 (2004)
- A.M. Taylor, S.W. Rhee, C.H. Tu, D.H. Cribbs, C.W. Cotman, N.L. Jeon, *Langmuir: ACS J Surfaces Colloids* **19**, 5 (2003)
- A.M. Taylor, M. Blurton-Jones, S.W. Rhee, D.H. Cribbs, C.W. Cotman, N.L. Jeon, *Nat. Methods* **2**, 8 (2005)
- A.M. Taylor, S. Menon, S.L. Gupton, *Lab Chip* **15**, 13 (2015)
- M. Tessier-Lavigne, M. Placzek, A.G.S. Lumsden, J. Dodd, T.M. Jessell, *Nature* **336**, 6201 (1988)
- C. Tsantoulas, C. Farmer, P. Machado, K. Baba, S.B. McMahon, R. Raouf, *PLoS One* **8**, 11 (2013)
- B. Vahidi, J.W. Park, H.J. Kim, N.L. Jeon, *J. Neurosci. Methods* **170**, 2 (2008)
- Y. Wang, V. Balaji, S. Kaniyappan, L. Krüger, S. Irsen, K. Tepper, et al., *Mol. Neurodegener.* **12** (2017)
- G.M. Whitesides, *Nature* **442**, 7101 (2006)
- Y. Yu, M.H. Shamsi, D.L. Krastev, M.D.M. Dryden, Y. Leung, A.R. Wheeler, *Lab Chip* **16**, 3 (2016)
- E.E. Zahavi, A. Ionescu, S. Gluska, T. Gradus, K. Ben-Yaakov, E. Perlson, *J. Cell Sci.* **128**, 6 (2015)